

## Finite element analysis of wellbore stability and optimum drilling direction and applying NYZA method for a safe mud weight window

Mohsen Heydari<sup>1</sup>, Mohammad Reza Aghakhani Emamqeyssi<sup>1</sup>, Manouchehr Sanei<sup>\*1</sup>  
 1- Department of Mining and Metallurgical Engineering, Yazd University, Yazd, Iran

\* Corresponding Author: *manouchehr.sanei@gmail.com*

(Received: July 2021 , Accepted: January 2022)

Keywords	Abstract
<b>Finite Element Method</b> <b>ABAQUS</b> <b>Wellbore Stability</b> <b>Drucker-Prager</b> <b>Mohr-Coulomb</b> <b>NYZA</b>	<p>Wellbore stability analysis, selecting the optimum drilling direction, and determining the safe and stable mud weight windows are among the major geomechanical challenges in the oil and gas industries. In this study, the wellbore stability analysis and the optimal drilling direction have been numerically modeled by the finite element method (FEM) considering the importance of wellbore stability and recognizing instabilities using the data of the Sivand oil field. The numerical modeling of wells behaviors has been performed in two modes of elastic and elastoplastic deformations using ABAQUS software. The numerical results have been done using the two failure criteria, namely Mohr-Coulomb and Drucker-Prager, and compared together, considering the effect of intermediate principal stress, Drucker-Prager failure criterion has been selected as a suitable failure criterion for this study. In addition, the numerical results have shown that the vertical well is the optimal drilling direction. Then, by applying the NYZA method, the safe mud weight window has been determined. The validity of the proposed mud window for a vertical well has been approved by applying the Mohr-Coulomb analytical method. Finally, a safe and stable mud window for the vertical wellbore has been proposed.</p>

### 1- Introduction

Wellbore stability analysis is an important part of a comprehensive operational study presented to minimize the risk of drilling operations and then decrease the costs associated with these operations in the petroleum industry. One of the main challenges in the drilling industry is to prevent the well breakouts and breakdowns. These problems can be controlled by choosing the appropriate drilling mud weight, suitable well casing design, and proper drilling method. Tensile and shear failures are among the most important instabilities that lead to mud loss, swelling, and wellbore collapse. These problems can be prevented by designing a suitable mud weight window. Wellbore collapse can cause several problems, including stuck pipe, wellbore closure, and the loss of drilling mud. Therefore, recognizing instabilities and trying to prevent them is essential in the oil and gas industry. The importance of wellbore stability analysis has been since 1979 and at the same time with Bradley's articles about wellbore breakout [1]. Then, in 1987, Adenoy and Chenworth presented the safe mud weight for the drilling of directional wells. In 1995, Morita et al. [2] identified pore pressure as one of the contributing factors in wellbore instability. Zoback et al. [3] found that shear failure occurs due to improper drilling mud pressure because if the mud exceeds a certain value and overcomes tensile strength, it can lead to drilling mud loss in the formations and induced tensile fractures in the well wall. Al-Ajmi and Zimmerman [4] designed a safe drilling mud

window to avoid the induced fracture around the wellbore and to decrease the induced stress concentration. Heydarian and Jalalifar applied the expansion of the plastic zone area as a basis for determining the safe mud window in underbalanced drilling operations. Li and Tang [5] proposed the optimal direction and the wellbore stability analysis based on the plastic zone around the wellbore. In addition, many studies have been performed to analyze wellbore stability based on numerical modelings, such as Coelho et al. [6] performed wellbore stability analysis with two-dimensional numerical modeling. Kaarstad and Aadnoy [7] and Al-Ajmi and Zimmerman [8] performed a wellbore stability analysis using three-dimensional numerical modeling. Sanei [9] proposed a wellbore stability analysis in the method of underbalanced drilling using FLAC<sup>3D</sup> software. Asgari et al. [10] analyzed the stability of the wellbore by applying the normalized yield zone area method, which was a method based on elastoplastic analysis. Recently, Behnam et al. [11] have numerically modeled the behavior of oil wells in Chile with a finite difference method using FLAC<sup>2D</sup> software. Garavand et al. [12] have also numerically modeled plastic deformations and fractures around wells by generalizing a two-dimensional model of plane strain conditions. Khodami et al. [13] have performed a 3D numerical modeling using ABAQUS software on the Maroon oilfield in southwestern Iran to analyze the effect of different parameters on the well cementing. Duran et al. [14] proposed an enhanced sequential fully implicit scheme for reservoir geomechanics in order to analyze the drilling of a wellbore in the linear and nonlinear

setting. Sanei et al. [15] developed a coupled poroelastoplasticity and permeability in order to analyze the wellbore instability problems during drillings such as pore collapse and shear enhanced compaction. Previous studies for wellbore stability have been emphasizing the importance of this problem. In addition, many oil and gas reservoirs are located in the anisotropic environment which requires a comprehensive analysis of wellbore stability. Therefore, in this study, the wellbore stability and selection of the optimal drilling direction have been presented by applying numerical modeling based on the finite element method. In addition, the importance of the normalized yield zone area method in determining the safe mud window based on the available information from one of the oil fields in southern Iran has been discussed. The following steps have been made in this research: first, the numerical modeling of the studied well has been performed using ABAQUS software based on two modes of elastic and elastoplastic analysis. Then, the verification of numerical models in the elastic state has been done by comparing the results with the analytical relationships. The elastoplastic analysis has been presented based on the Drucker-Prager and Mohr-Coulomb criteria. Next, according to the numerical results, the appropriate yield criterion for the next analysis, such as optimal drilling direction has been chosen. Then, the safe mud window has been determined using numerical results by considering the normalized yield zone area method. Afterward, the validation of the safe mud window for a vertical well has been evaluated using the Mohr-Coulomb analytical method. Finally, the safe and stable mud window for the vertical wellbore has been presented.

## 2- Methodology

### 2-1- Wellbore instability problems

The most key point for analyzing wellbore stability is to recognize the factors and indicators affecting wellbore instability. The knowledge about these factors as listed in Table 1 helps to prevent wellbore instability. The indicators of wellbore instability are divided into direct and indirect parts. A list of these indicators that cause the wellbore instability during drilling and completion is given in Table 2.

**Table 1. Factors of Wellbore Instability [16]**

Uncontrollable Factors	Controllable Factors
Naturally Fractured	Bottom Hole Pressure
Tectonically Stressed Formations	Well Inclination and Azimuth
High In-situ Stresses	Transient Pore Pressures
Mobile Formations	Erosion
Unconsolidated Formations	Physic/chemical Rock-Fluid Interaction
Naturally Over-Pressured Shale Collapse	Drill String Vibrations
Induced Over-Pressured Shale Collapse	Temperature

**Table 2. Indicators of wellbore instability [17]**

Direct indicators	Indirect indicators
Oversize hole	High torque and drag
Under gauge hole	Hanging up of drill string, casing, or coiled tubing
Excessive volume of cuttings	Increased circulating pressures
Excessive volume of cavings	Stuck pipe
Cavings at surface	Excessive drill string vibrations
Hole fill after tripping	Drill string failure
Excess cement volume required	Deviation control problems
	Inability to run logs
	Poor logging response
	Annular gas leakage due to poor cement job
	Keyhole seating
	Excessive doglegs

### 2-2- In-situ stresses magnitude

The in-situ stresses are important parameters decision making about different stages of drilling and analyzing the wellbore stability. The correct estimation of in-situ stresses can be useful to different problems in the oil and gas industry, such as effective drilling direction, optimum hydraulic fracture, wellbore stability, sand production, etc. The amount of vertical in-situ stress ( $S_v$ ) due to the weight of the upper layer can be computed using Equation 1 [18]:

$$S_v = \int_0^z \rho(z)g dz \approx \bar{\rho}gz \quad (1)$$

where  $z$  is the depth,  $\rho_z$  is the density of the rock as a function of depth,  $g$  is the acceleration of gravity, and  $\bar{\rho}$  is the average density of the overburden weight.

The poroelastic equations (Eq. 2 and 3) can be used to compute the minimum ( $S_h$ ) and maximum ( $S_H$ ) horizontal stresses [19]:

$$S_h = \frac{v}{(1-v)}(S_v - \alpha P_p) + \alpha P_p + \frac{E_s}{(1-v^2)}\varepsilon_x + \frac{v \times E_s}{(1-v^2)}\varepsilon_y \quad (2)$$

$$S_H = \frac{v}{(1-v)}(S_v - \alpha P_p) + \alpha P_p + \frac{E_s}{(1-v^2)}\varepsilon_y + \frac{v \times E_s}{(1-v^2)}\varepsilon_x \quad (3)$$

where  $\nu$  is Poisson's ratio,  $S_v$  is the vertical stress,  $\alpha$  is the Biot coefficient,  $P_p$  is the pore pressure,  $E_s$  is the static Young modulus. The amount of tectonic strain in the X ( $\varepsilon_x$ ) and Y ( $\varepsilon_y$ ) directions can be determined using Equations 4 and 5 [19]:

$$\varepsilon_x = \frac{S_y \times v}{E_s} \left( \frac{1}{1-v} - 1 \right) \quad (4)$$

$$\varepsilon_y = \frac{S_y \times v}{E_s} \left( 1 - \frac{v^2}{1-v} \right) \quad (5)$$

### 2-3- Elastoplastic constitutive models

The elastoplastic deformation of the rock can be described based on the theory of elastoplasticity for materials that undergo permanent deformation under certain loading conditions. In this study, the elastoplastic deformation of the rock has been described using Drucker–Prager and Mohr-Coulomb criteria.

### 2-4- Drucker-Prager criterion

The Drucker-Prager yield criterion, presented as a generalization of the Mohr-Coulomb criterion for soil, includes the modification of the Von-Mises criterion, which is expressed as follows [20]:

$$f(P, \sqrt{J_2}) = \sqrt{J_2} + \eta P - \xi c \tag{6}$$

where  $P$  is the hydrostatic component of the stress tensor,  $J_2$  is the second invariant of the stress deviator tensor,  $c$  is the cohesion, and the constant parameters  $\eta, \zeta$  are selected according to the required approximation of the Mohr-Coulomb model. The values of the parameters  $\eta$  and  $\zeta$  are equal to:

$$\eta = \frac{6 \sin \varphi}{\sqrt{3}(3 - \sin \varphi)} \tag{7}$$

$$\xi = \frac{6 \cos \varphi}{\sqrt{3}(3 - \sin \varphi)} \tag{8}$$

where  $\varphi$  is the friction angle.

### 2-3-2 Mohr-Coulomb criterion

The Mohr-Coulomb yield criterion occurs when the shear strength  $\tau_m$  and normal stress  $\sigma_n$  reach a critical combination as follows [21, 22]:

$$\tau_m = c + \sigma_n \tan \varphi \tag{9}$$

where  $c$  is the cohesion and  $\varphi$  is friction angle.

### 2-5- Optimum mud window

Determining the drilling mud window is one of the essential steps to analyze the stability of the wellbore. This step can be performed by considering the geo-mechanical modeling of well drilling. In this method, the safety mud pressure must be designed and chosen in such a way as to prevent the induced natural fractures, induced tensile cracks during drilling, and wellbore instability. As illustrated in Fig. 1, the mud pressure is acceptable for safe and stable drilling in the breakout pressure and horizontal minimum stress range ( $S_3$ ). There are several methods to evaluate the wellbore stability, which are being mentioned below.

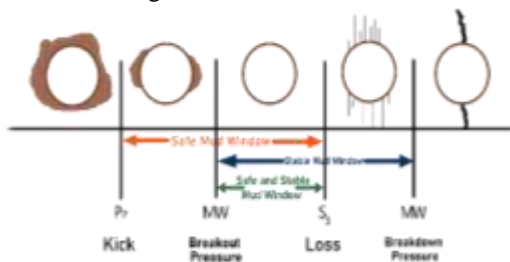


Fig. 1. A schematic of wellbore stability and instability intervals

### 2-4-1 Normalized yield zone area method

A method to determine the range of mud pressure under elastoplastic conditions is to use the normalized yield zone area (NYZA) variable. In this method, as shown in Fig. 2, the value of NYZA can be obtained by dividing the plastic area ( $A_1$ ) by the area of the initial cross-section of the well ( $A_2$ ).

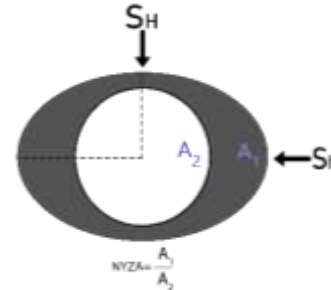


Fig. 2. Schematic representation of NYZA concept

As expressed by Hawkes and McLellan [23] for the elastoplastic conditions the wellbore stability is done when NYZA is equal to 1. In other words, for wellbore stability, the range of mud pressure applied to the well is such that the NYZA value is less than 1. If the NYZA value exceeds the value of 1, it will lead to serious problems in drilling operations and consequently wellbore instability [11]. Therefore, it can be concluded that to avoid shear failure, the value of NYZA = 1 is considered the critical limit.

### 2-4-2- Mohr-Coulomb analytical method

The Mohr-Coulomb method can be applied to evaluate wellbore stability and to determine safe drilling mud pressure. In this method, using the Mohr-Coulomb criterion and calculating the stresses around the well, the mud pressure can be presented. The stresses at a vertical wellbore wall, according to the Kirsch solution (Eq. 10), are obtained as [8,24]:

$$\begin{aligned} \sigma_r &= P_w \\ \sigma_\theta &= S_H + S_h - 2(S_H - S_h)\cos 2\theta - P_w \tag{10} \\ \sigma_z &= S_v - 2\nu(S_H - S_h)\cos 2\theta \end{aligned}$$

where  $\sigma_r$  is the radial stress,  $\sigma_\theta$  is the tangential stress,  $\sigma_z$  is the axial stress,  $P_w$  is the internal wellbore pressure, and  $\nu$  is the Poisson ratio of the rock. The angle  $\theta$  is measured clockwise from the  $\sigma_H$  direction (x-axis). Radial and tangential stresses are a function of  $P_w$ , therefore when  $P_w$  decreases,  $\sigma_\theta$  increases. The lower limit of the mud pressure,  $P_{wb}$ , is associated with breakout, in which  $\sigma_\theta$  should be greater than  $\sigma_r$ . There are three permutations of the principal stresses that need to be investigated in order to determine the minimum allowable mud pressure: (1)  $\sigma_z \geq \sigma_\theta \geq \sigma_r$ , (2)  $\sigma_\theta \geq \sigma_z \geq \sigma_r$ , and (3)  $\sigma_\theta \geq \sigma_r \geq \sigma_z$ . The compressive strength of the rock in the case of the maximum value of stress  $\sigma_\theta$  or  $\sigma_z$  (i.e.,  $\theta = \pm\pi/2$ ) has the highest value, thus, the corresponding principal stresses at the wellbore wall become [8]:

$$\begin{aligned}\sigma_r &= P_w \\ \sigma_\theta &= A - P_w \\ \sigma_z &= B\end{aligned}\quad (11)$$

where A and B are given by [8]:

$$\begin{aligned}A &= 3S_H - S_h \\ B &= S_v + 2v(S_H - S_h)\end{aligned}\quad (12)$$

After determining the wellbore wall stresses, the Mohr-Coulomb failure criterion should be used to determine the safe mud pressure. In this case, according to the concept of effective stress, the Mohr-Coulomb failure criterion is given by [8]:

$$\sigma_1 = C_0 + q\sigma_3 \quad (13)$$

$$C_0 = c - P_0(q - 1) \quad (14)$$

where  $C_0$  is the uniaxial compressive strength,  $P_0$  is the pore pressure and  $q = (1 + \sin\varphi)/(1 - \sin\varphi)$  can be related to the internal friction  $\varphi$  and cohesion ( $c$ ). According to the Mohr-Coulomb failure criterion, the safe mud pressure corresponding to the wellbore pressure ( $P_{wb}$ ) for three of the major stresses is listed in Table 3; in this case, breakout can occur when  $P_w \leq P_{wb}$ .

**Table 3. The mohr-Coulomb criterion for breakout pressure in vertical wellbores [8]**

Case	$\sigma_1 \geq \sigma_2 \geq \sigma_3$	$P_{wb}$
1	$\sigma_z \geq \sigma_\theta \geq \sigma_r$	$P_{wb1} = (B - C)/q$
2	$\sigma_\theta \geq \sigma_z \geq \sigma_r$	$P_{wb2} = (A - C)/(1 + q)$
3	$\sigma_\theta \geq \sigma_r \geq \sigma_z$	$P_{wb3} = A - C - qB$

### 3- Characteristics of the study area

This research has been done based on the data from the Iran Sivand oil field located 100 (km) of the southern coasts of Iran in the Persian Gulf. This field is located 33 (km) southwest of Siri Island and 14 km northwest of Esfand field. The anticline of this field consists of Ilam, Sarvak, and Darian formations. Also, the total number of wells in this field is 33, of which 24 wells have been completed as production wells. Fig. 3, shows the location of the Sivand oil field.



**Fig. 3. Location of the Sivand oil field**

The geomechanical data and fluid flow characteristics of the Sivand oil field are given in Tables 4 and 5. The quantities of in-situ stresses are obtained according to the Eqs. (1) TO (5), and they are presented in Table 6.

**Table 4. Geo-mechanical characteristics of the Sivand oil field**

Parameter	Magnitude
$\sigma_c$ (MPa)	30.19
cohesion (MPa)	6.72
Friction Angle $\varphi$ (Degree)	42
Biot Coefficient $\alpha$	0.7
Poisson's ratio $\nu$	0.29
Young's Modulus (GPa)	28.38
Specific weight $\gamma$ (g/cm <sup>3</sup> )	2.72

**Table 5. Fluid flow characteristics of the Sivand oil field**

Parameter	Magnitude
Pore Pressure (MPa)	15
Oil density (g/cm <sup>3</sup> )	0.68
Permeability (md)	18.7
Porosity (%)	23.4

**Table 6. In-situ stresses of the Sivand oil field**

Parameter	Magnitude
$S_v$ (MPa)	67.1
$S_H$ (MPa)	54.9
$S_h$ (MPa)	47.7

### 4- Numerical modeling

#### 4-1- Finite element method

The finite element method (FEM), is the most common numerical method for solving engineering problems. In this method, to solve a problem, the FEM subdivides a large system into smaller parts which are called finite elements. It is done by a special space discretization in the space dimensions. The spatial discretization is obtained by meshing the domain. The finite element method formulation of a boundary value problem finally becomes a system of algebraic equations that represents approximations of the unknown function over the domain [25]. The equations that model the finite elements are then assembled into a larger system of equations that models its entire. The FEM approximation is obtained by minimizing the error estimation.

ABAQUS software is one of the most powerful engineering software used in finite element analysis (FEM). This software has a wide set of elements that any kind of geometry can be modeled with these elements. It also has many material models that make it possible to model a variety of materials with different properties and behaviors [26].

#### 4-2- Numerical modeling of well

In this research, wellbore modeling has been done based on finite element numerical method using ABAQUS software. The wellbore under study, as shown in Fig. 4, has a diameter of 0.2032 meters, and due to the macro-geo-mechanical view, the dimensions of the numerical model are considered 100 times the diameter of the well to prevent the effect of stress distribution on the boundaries. According to the assumption of double symmetry of the problem to reduce the analysis time, only a quarter of the geometry is modeled. After making the geometry of the model, the material properties of the model, the boundary conditions, in-situ stresses, and wellbore pressure resulting from the mud weight are applied until the model reaches equilibrium. Since the problem is poroelastic, the stress quantities are applied as effective stresses to consider the pore pressure effect. In order to increase the accuracy of computation, the geometry of the model is divided into three parts; the mesh size changes from the wellbore wall to the model boundaries respectively  $20 * 15, 15 * 15$ , and  $18 * 15$ . The plane strain condition is applied in this model.

In this research, both linear elastic and elastoplastic modes have been used to evaluate the wellbore stability. One of the limitations of the linear elastic model is that when the stresses around the well reach the yield point of the rock, the rock will completely lose its strength. While the rock is weakened after the yield point and doesn't have the initial resistance, the residual resistance prevents the rock from its failure completely through the plastic area. The size of the plastic area plays an important role in the wellbore stability. Therefore, the evaluation of wellbore stability using the elastoplastic method is more realistic than the linear elastic method [10].

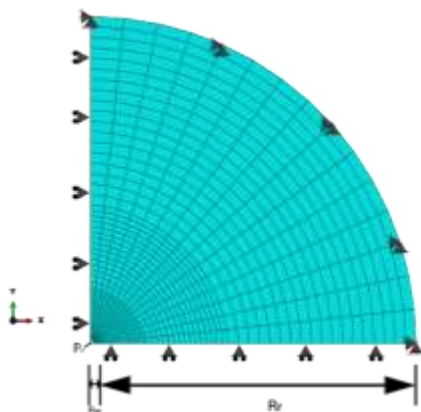


Fig. 4. The boundary conditions of the well

#### 5- Results and Discussion

The numerical results are divided into two modes: elastic and elastoplastic. The results include maximum stress (S11), minimum stress (S22), displacement along the x-axis (U1), and displacement along the Y-axis (U2). The numerical results of the elastic state are compared with the analytical equations related to radial stress and displacement to verify the accuracy of the model. In addition, the numerical modeling in the elastoplastic state considering the Drucker-Prager and Mohr-Coulomb criterion has been generated under similar loading and boundary conditions in the elastic state. In this case, the numerical results of the two mentioned criteria are compared with each other to select the optimum criterion for determining the drilling mud window. Then, the mud weight window is calculated based on the normalized yield zone area (NYZA) and the Mohr-Coulomb analytical method. Finally, the importance of the NYZA method to determine the safe mud weight window of drilling is mentioned.

##### 5-1- Elastic results

In order to model in the elastic state, two material parameters, namely, Young's modulus and Poisson's ratio are used. After applying these parameters and setting the boundaries and loading conditions, the results are obtained for both horizontal and vertical well modes. The numerical modeling has been performed by considering underbalanced drilling. The numerical results, as shown in Figs. 5 to 8, include maximum and minimum stresses in the vertical well, displacement along the X and Y axes in the vertical well, maximum and minimum stresses, and displacement in the horizontal wellbore.

Since similar results have been obtained along the reservoir radius, in the above figures only a part of the reservoir radius has been chosen to present the results around the wellbore. As expected, the intensity of induced stress around the wellbore is more than the stress far from the well, and with increasing the distance from the well, the amount of induced stresses decreases, and finally at the outer boundary of the model, the amount of stresses approaches to the in situ stresses. As shown in Fig. 5(a) and Fig. 7(a), the maximum stress value is along the Y-axis and the minimum stress value is along the X-axis. In addition, as displayed in Fig. 6 and Fig. 8, the displacement near the vertical and horizontal wells are about 0.1% and 0.2% of the diameter of the wellbore, respectively, and as the distance far from the wellbore, the displacement will be zero.



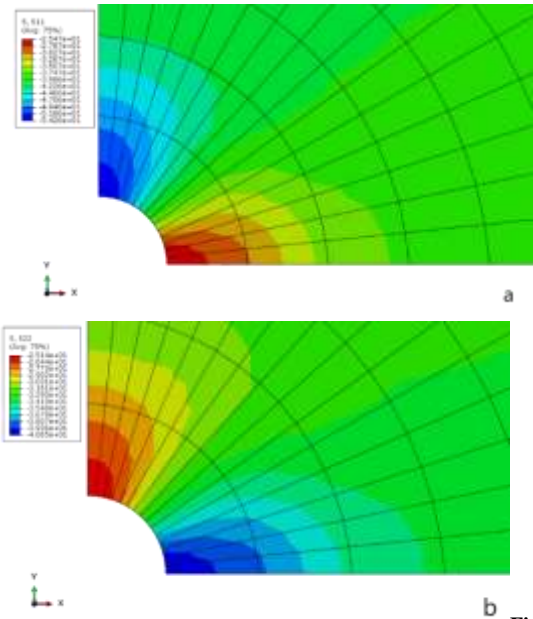


Fig.

5. Results of Stresses, (a) S11 and (b) S22 in vertical well SS

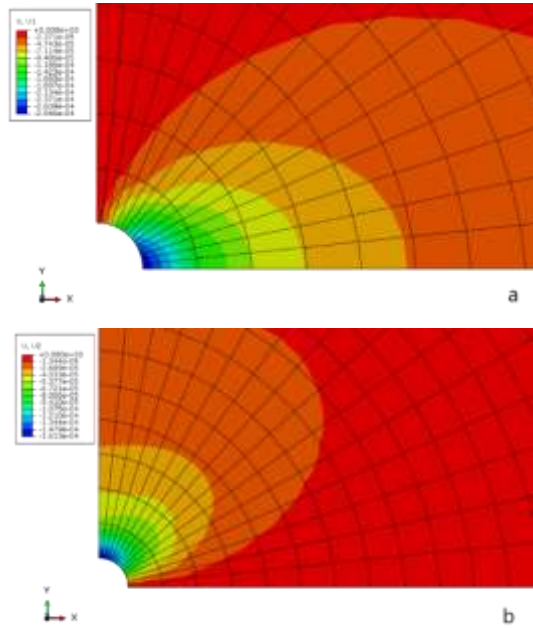


Fig. 6. Displacement results in the (a) X-axis and (b) Y-axis in the vertical well

### 5-2- Verification of elastic results

To verify the numerical results in the elastic state, analytical relationships are used. These equations have been presented for stress and displacement in the fully drained conditions, as written about stress as [27]:

$$\sigma_r = \frac{S_h + S_H}{2} \left( 1 - \frac{R_w^2}{r^2} \right) + \frac{S_h - S_H}{2} \left( 1 + 3 \frac{R_w^4}{r^4} - 4 \frac{R_w^2}{r^2} \right) \cos 2\theta + \frac{R_w^2}{r^2} P_w \quad (15)$$

where  $r$  is the radial distance from the wellbore,  $\theta$  is the direction that is considered zero in this study,  $P_w$  is the wellbore pressure,  $R_w$  is the wellbore radius,  $S_H$  and  $S_h$  are the maximum and minimum horizontal stress, respectively.

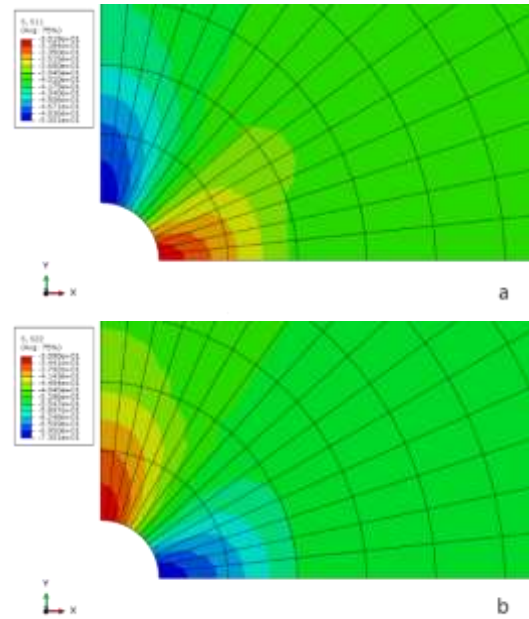


Fig. 7. Results of Stresses, (a) S11 and (b) S22 in horizontal well

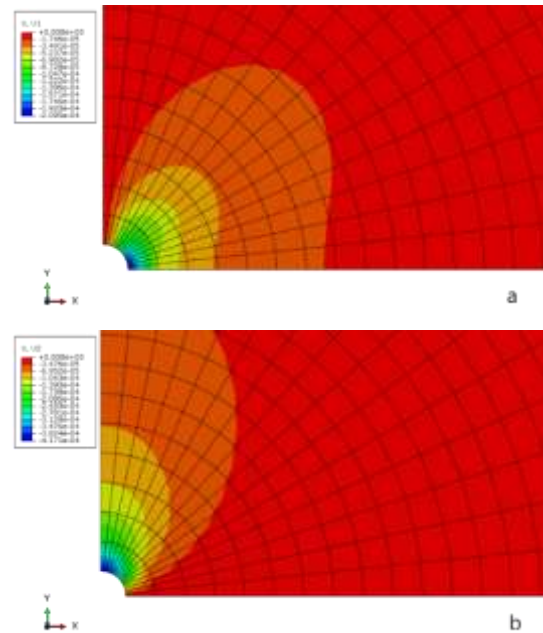


Fig. 8. Displacement results in the (a) X-axis and (b) Y-axis in horizontal well

The radial displacement is calculated using the following equation [27]:

$$U_d = \frac{S_h - P_w}{2G} \frac{R_w^2}{r} \quad (16)$$

where  $G$  is the shear modulus which is computed using Young's modulus  $E$  and Poisson's ratio  $\nu$  through the following equation [27]:

$$G = \frac{E}{2(1+\nu)} \quad (17)$$

After implementing the numerical modeling, we compare the numerical results of our implementation with the above analytical solutions for radial stress and displacement. The mentioned comparatives for stress and displacement around the wellbore are shown in Fig. 9.

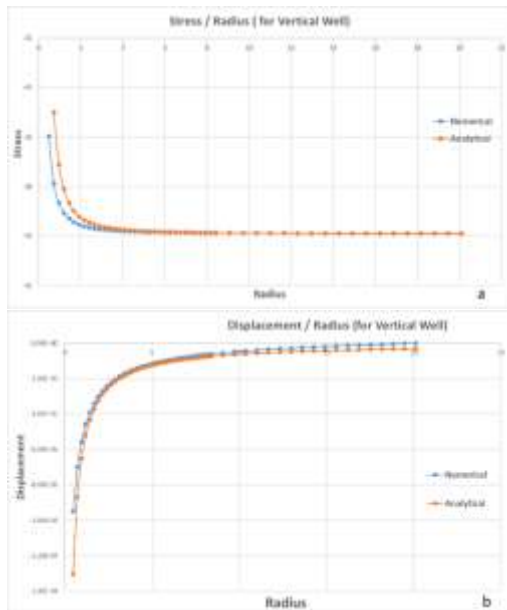


Fig. 9. The plot of (a) stress and (b) displacement around the vertical wellbore

All the subfigures in Fig. 9 illustrate a comparison for the numerical modeling with the results calculated from analytical solutions (see Eq. 15 and 16), demonstrating the verification of the implementation for stress and displacement around the wellbore in the elastic state. This verification can also be done for the elastoplastic state using Runge-Kutta solver as the same scheme presented by Duran et al. [14] and Sanei et al. [28].

### 5-3- Elastoplastic results

After verification of numerical modeling in the elastic state, the numerical modeling extends to the elastoplastic state. Due to the importance of choosing the appropriate direction of drilling, it is essential to implement the numerical modeling based on geomechanical and tectonic parameters before each drilling operation to analyze the different drilling directions in order to select the optimum one. Therefore, in this study, the optimum direction of wellbore drilling is investigated among vertical well, horizontal well along maximum horizontal stress, and horizontal well along minimum horizontal stress. The numerical modeling of wellbore stability is performed based on two Mohr-Coulomb and Drucker-Prager criteria. The choice of these two criteria has been made in order to present the effect of intermediate stress on the wellbore stability. As expressed in previous studies, the Mohr-Coulomb yield criterion ignores the effect of the intermediate stress, and the Drucker-Prager criterion considers its effect [29]. The numerical results, as displayed in Fig. 10, show that the plastic zone with the Mohr-Coulomb criterion is much larger than the Drucker-Prager criterion. These results are similar to previous studies expressed by Hassani Zaveh et al. [29] and Wang et al. [30]. They performed wellbore stability and compared the results of Mohr-Coulomb and Drucker-Prager criteria together. The

results of them showed that the Drucker-Prager criterion has more acceptable results. Therefore, according to the similarity of the numerical results of this study with mentioned references [29, 30], the Drucker-Prager yield criterion is selected as the appropriate one. As expressed above, the Drucker-Prager criterion is the optimal one, thus the following numerical modeling in the elastoplastic state is done based on this criterion. To be able to select the optimum direction of drilling, the numerical modeling is done separately for the three different conditions, namely vertical wellbore, horizontal wellbore in the direction of minimum and maximum horizontal stress. The numerical results are reported for each condition in the appendix that includes stresses (S11) and (S22) as well as displacements (U1) and (U2). The numerical results as presented in the appendix show that the vertical well is the optimum direction of drilling because the induced stresses around the vertical wellbore are much lower compared to other directions.

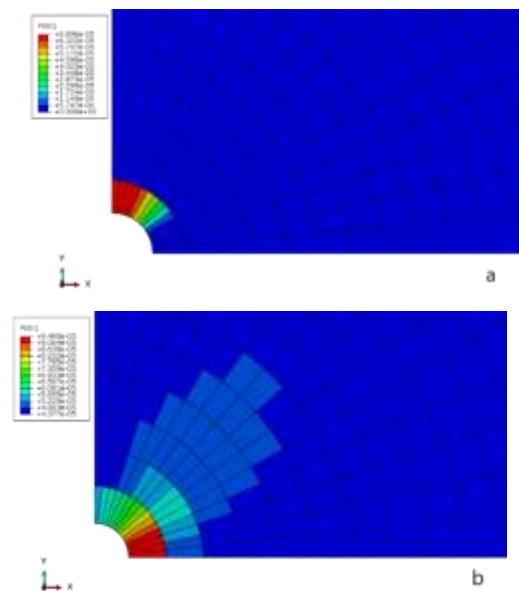


Fig. 10. The plastic zone around the well with yield criteria: (a) Drucker-Prager, (b) Mohr-Coulomb

### 5-4- Determination of mud pressure

The wellbore stability analysis and determination of the mud weight window can be done using numerical modeling and the NYZA method. As mentioned in Section 2-4-1, the NYZA method can be used to determine the mud pressure window. This method is based on the ratio between the plastic area ( $A_1$ ) to the initial cross-sectional area of the well ( $A_2$ ). In this study, different quantities of wellbore pressures are considered to compute mud pressure window using the NYZA method. The area of the plastic zone surface after each implementation is estimated using the AutoCAD software. Then, the NYZA is obtained by dividing the plastic zone area to the area of the wellbore. The results of computing NYZA are shown in Fig. 11.

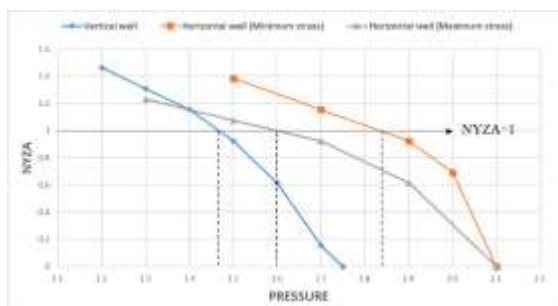


Fig. 11. Results of NYZA under different pressures

The NYZA method is applied for three different conditions such as vertical well, horizontal well in the direction of minimum horizontal stress, and horizontal well in the direction of maximum horizontal stress. According to the numerical results obtained from the NYZA method, when a well is drilled vertically, the value of NYZA at a mud pressure of 14.6 MPa is equal to 1. As regards  $NYZA = 1$  is considered as the threshold, the minimum mud pressure that can be safe in the vertical well is 14.6 Mpa. In addition, when the well is drilled in the direction of maximum and minimum horizontal in-situ stress, the values of minimum mud pressure for safe drilling are 16 and 18.3 MPa, respectively.

Moreover, the mud pressure can be determined using an analytical method. As shown in Fig. 1, three different mud windows, including safe mud window, safe and stable mud window, and stable mud window can be defined for the amount of mud weight. In this study, to determine the safe mud window for vertical wells, the Mohr-Coulomb analytical method, which was described in Section 2-4-2, is used. After computing the stresses around a vertical wellbore using equations 10 to 14 and comparing the results, it is concluded that the values of stresses around the well are in the form  $\sigma_{\theta} \geq \sigma_z \geq \sigma_r$ . Then, by evaluating the relationships in Table 3, it is obtained that the second relationship is a suitable one for calculating the lower limit of the safe and stable mud window. The breakout pressure is obtained using the second relationship that is equal to 19.43 Mpa. Moreover, the upper limit of the safe and stable mud window as presented in Fig. 1 is the value of horizontal minimum stress, namely 32.7 MPa. According to that, the range of 19.43 to 32.7 Mpa is the safe and stable mud window, in addition, the other mud window is the safe mud window in which the lowest limit of the mud pressure window is equal to pore pressure, namely 15 MPa and its upper limit is equal to horizontal minimum stress, namely 32.7 MPa. Finally, the ideal interval for the mud weight window for the vertical wellbore is proposed based on the safe and stable mud window, namely the range of 19.43 to 32.7 MPa because it causes much less damage around the wellbore.

## 6- Conclusion

According to the numerical modeling performed in two modes of elastic and elastoplastic, as well as the

determination of the mud window, the following results have been obtained from this study:

- By computing the results in the elastic state numerically and analytically and comparing the data with each other, it was concluded that the data obtained from the numerical and analytical methods are very close to each other and it can be expressed that the results obtained from the numerical method are valid.
- Considering the comparison of the numerical modeling based on the Mohr-Coulomb and Drucker-Prager criteria, it showed that the results of the Drucker-Prager criterion in the plastic state are closer to reality.
- The obtained results from the induced stresses and displacements in the elastoplastic state using numerical modeling illustrated that the vertical well is the optimal direction for the wellbore drilling.
- The safe mud pressure window determined by the normalized yield zone area method has been less for the vertical well compared to the other directions, namely the direction of horizontal minimum and maximum stress; therefore, drilling wells in the vertical direction is better in terms of stability and economy.
- By computing the drilling mud window using the Mohr-Coulomb analytical method and comparing the results with the values obtained from the NYZA method and numerical modeling, it was concluded that the mud window range based on all three methods are close to each other and also the safe and stable mud window for the vertical wellbore is equal to 19.43 to 32.7 MPa.

## REFERENCES

- [1] Bradley W. Failure of inclined boreholes. 1979.
- [2] Morita N, editor Uncertainty analysis of borehole stability problems. SPE Annual Technical Conference and Exhibition; 1995: Society of Petroleum Engineers.
- [3] Zoback MD. Reservoir Geomechanics: Cambridge University Press; 2010
- [4] Al-Ajmi AM, Zimmerman RW. A new well path optimization model for increased mechanical borehole stability. Journal of Petroleum Science and Engineering. 2009;69(1-2):53-62.
- [5] Li Q, Tang Z. Optimization of borehole trajectory using the initial collapse volume. Journal of Natural Gas Science and Engineering. 2016;29:80-8.
- [6] Coelho LC, Soares AC, Ebecken NFF, Alves JLD, Landau L. The impact of constitutive modeling of porous rocks on 2-D wellbore stability analysis. Journal of Petroleum Science and Engineering. 2005;46(1-2):81-100.
- [7] Kaarstad E, Aadnoy BS, editors. Optimization of borehole stability using 3-D stress optimization. SPE annual technical conference and exhibition; Society of Petroleum Engineer, 2005.
- [8] Al-Ajmi AM, Zimmerman RW. Stability analysis of vertical boreholes using the Mogi-Coulomb failure



criterion. International Journal of Rock Mechanics and Mining Sciences. 2006;43(8):1200-11.

[9] Sanei, M. 2011. Wellbore stability analysis in the method of under balanced drilling, in: Proceeding of the 8th Iranian Student Conference of Mining Engineering; Tehran, Iran. (In Persian).

[10] Asgari, Ramin, Haydarizadeh, Meamarian. Analysis of wellbore stability and Determination of Mud weight window with NYZA at a South oil field. Exploration and production oil and GAS. 2017;1396(146):59-65. (In Persian).

[11] Behnam N, Hosseini M, Shahbazi S. A Criterion for Estimating the Minimum Drilling Mud Pressure to Prevent Shear Failure in Oil Wells. Geotechnical and Geological Engineering. 2020;38(1):227-36. (In Persian).

[12] Garavand, A., Stefanov, Y. P., et al. "Numerical modeling of plastic deformation and failure around a wellbore in compaction and dilation modes." International Journal for Numerical and Analytical Methods in Geomechanics. 2020;44(6):823-50

[13] Khodami, E., Ramezanzadeh, A., et al. "Numerical modeling of oil well integrity with a particular view to cement (case study: Maroon Oilfield in southwest of Iran)." Journal of Petroleum Science and Engineering. 2021;196:107991.

[14] Duran, O., Sanei, M., Devloo, P. Santos, E. 2020. An enhanced sequential fully implicit scheme for reservoir geomechanics. Journal of Computational Geosciences.

[15] Sanei, M., Duran, O., Devloo, P., Santos, E. 2021. Analysis of pore collapse and shear-enhanced compaction in hydrocarbon reservoirs using coupled poro-elastoplasticity and permeability. Arabian Journal of Geosciences.

[16] McLellan, P. J., Wang, Y. "Predicting the effects of pore pressure penetration on the extent of wellbore instability: Application of a versatile poro-elastoplastic model." Rock Mechanics in Petroleum Engineering; 1994. SPE-28053-MS.

[17] Pašić, B., Gaurina-Međimurec, N., et al. "Wellbore instability: Causes and consequences." Rudarsko-Geološko-Naftni Zbornik. 2007;19.

[18] Zang, A., Stephansson, O. "Rock fracture criteria. Stress Field of the Earth's Crust: Springer; 2010. p. 66.

[19] Najibi, A. R., Ghafoori, M., et al. "Reservoir geomechanical modeling: In-situ stress, pore pressure, and mud design." Journal of Petroleum Science and Engineering. 2017;151:31-9.

[20] Drucker DC, Prager W. Soil mechanics and plastic analysis or limit design. Quarterly of applied mathematics. 1952;10(2):157-65.

[21] Mohr O. Welche Umstände bedingen die Elastizitätsgrenze und den Bruch eines Materials. Zeitschrift des Vereins Deutscher Ingenieure. 1900;46(1524-1530):1572-7.

[22] Coulomb CA. Essai sur une application des regles de maximis et minimis a quelques problemes de statique relatifs a l'architecture (essay on maximums and minimums of rules to some static problems relating to architecture). 1973.

[23] McLellan P, Hawkes C. Borehole Stability Analysis for Underbalanced Drilling. Journal of Canadian Petroleum Technology. 2001;40(05).

[24] Kirsch, C. "Die theorie der elastizitat und die bedürfnisse der festigkeitslehre." Zeitschrift des Vereines Deutscher Ingenieure. 1898.

[25] Logan DL. A First Course in the Finite Element Method: Cengage Learning; 2011.

[26] Manual of Abaqus/CAE Version: 6.14-2, Dassault Systèmes Simulia Corp. 2014.

[27] Fjar E, Holt RM, Raaen AM, Horsrud P. Petroleum Related Rock Mechanics: Elsevier Science; 2008.

[28] Sanei, M., Duran, O., Devloo, P. Santos, E. Evaluation of the impact of strain-dependent permeability on reservoir productivity using iterative coupled reservoir geomechanical modeling, (Geomechanics and Geophysics for Geo-Energy and Geo-Resources), January, 2022.

[29] Hassani Zaveh SR, Ahmadi M, Ghoreishian Amiri SA. An Elastic-Perfect Plastic Constitutive Model Based on Mogi-Coulomb Yield Criterion. Journal of Analytical and Numerical Methods in Mining Engineering. 2018;7(14):51-9. (In Persian).

[30] Wang, J., Weijermars, R. "New Interface for Assessing Wellbore Stability at Critical Mud Pressures and Various Failure Criteria: Including Stress Trajectories and Deviatoric Stress Distributions." Energies. 2019;12(20):4019.

## Appendix

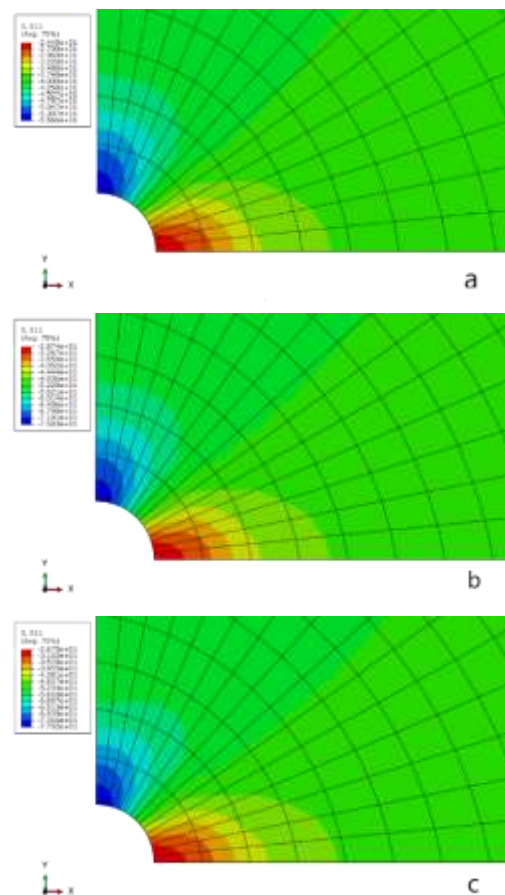


Fig. 12. S11 stress output in the elastoplastic state in (a) vertical well, (b) horizontal well in the direction of minimum horizontal stress, (c) horizontal well in the direction of maximum horizontal stress

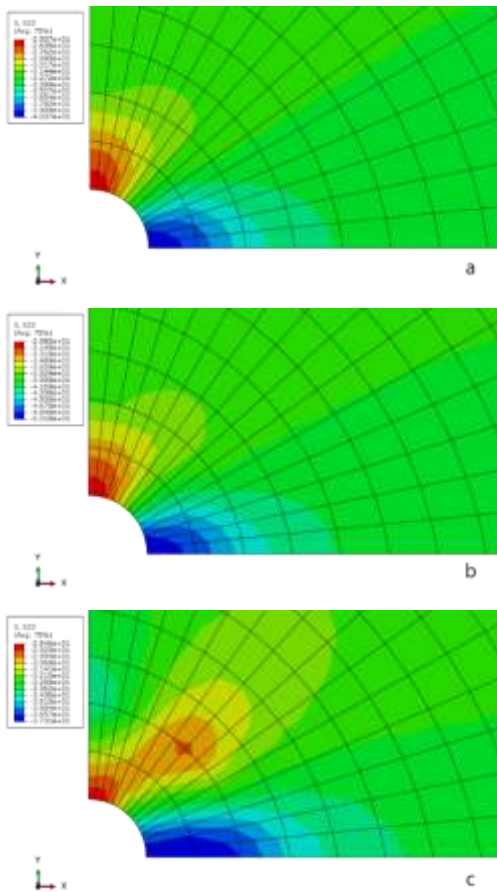


Fig. 13. S22 stress output in the elastoplastic state in (a) vertical well, (b) horizontal well in the direction of minimum horizontal stress, (c) horizontal well in the direction of maximum horizontal stress

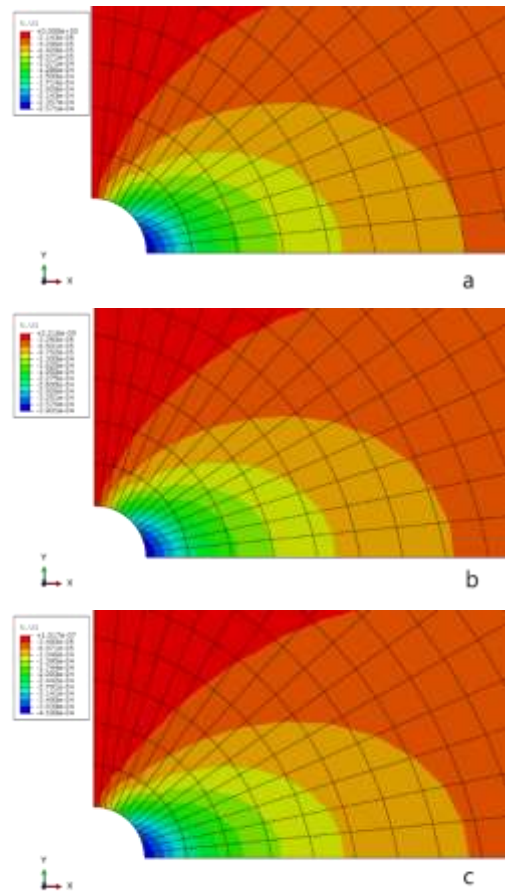


Fig. 14. Results of U1 displacement in the elastoplastic state in (a) vertical well, (b) horizontal well in the direction of minimum horizontal stress, (c) horizontal well in the direction of maximum horizontal stress

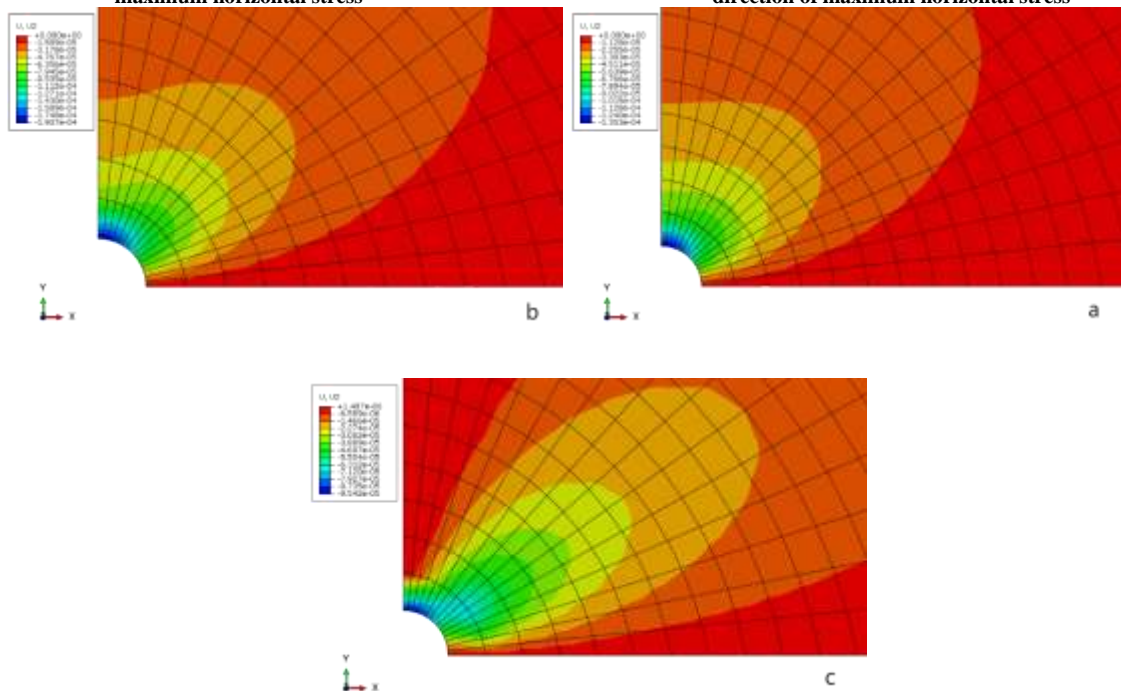


Fig. 15. Results of U2 displacement in the elastoplastic state in (a) vertical well, (b) horizontal well in the direction of minimum horizontal stress, (c) horizontal well in the direction of maximum horizontal stress